Numerical Investigation on Mechanical Behaviour of Natural Barrier in Geological Repository of High-Level Radioactive Waste

Y. Kurimoto[1], Y. L. Xiong[2], S. Kageyama[1] and F. Zhang[1]
[1]*Department of Civil Engineering, Nagoya Institute of Technology, Nagoya, Japan*
[2]*Department of Geotechnical Engineering, Tongji University, Shanghai, China*
E-mail: cho.ho@nitech.ac.jp

ABSTRACT: It is commonly known that geological repository is regarded as the most practical way of permanent disposal of high-level radioactive waste (HLW). Yet, there are some engineering problems needed to be solved before its practical application. In geological repository, one of the most important factors is the thermo-hydraulic-mechanical (THM) behaviour of natural barrier. The aim of this paper is to investigate the influence of temperature on the deformation and the strength of host rocks, such as the soft sedimentary rock, with some element tests and the numerical simulations with a program of FEM named as ***SOFT*** based on a thermo-elasto-viscoplastic constitutive model.

Keywords: Soft sedimentary rock, Geological repository of HLW, Thermo-hydraulic-mechanical coupling

1. INTRODUCTION

In Japan, nuclear electricity generation had occupied about 30% of total power generation until the nuclear accident at the Tokyo Electric Power Company's Fukushima No.1 nuclear power on March 11, 2011. Using the nuclear electricity generation forces us to face with serious problems of how to manage the nuclear waste disposal, especially the repository of high-level radioactive waste (HLW). Nowadays, the deep geological repository is regarded as one of the most viable and practical way of permanent disposal of HLW (Japan Nuclear Cycle Development Institute, 2000). The soft sedimentary rock is considered as a suitable natural barrier for the geological repository of HLW. In reality, however, the amount of thermal energy generated by HLW is huge enough to damage the environment and human society and would last for hundreds years (Thunvik and Braester, 1991; Japan Nuclear Cycle Development Institute, 2000). Some long-lived radionuclides may even affect the environment, more or less, much longer. It is known that the temperature and its change may affect the mechanical behaviour of the soft sedimentary rock, especially the long-term stability. Cyclic water absorption-evaporation processes may also lead to swelling and slaking of not only the engineered barrier but also the natural barrier because the buffer material is usually unsaturated during initial period, and will be subjected to hydration from the natural barrier. It is therefore absolutely necessary to study carefully the thermo-hydraulic-mechanical (THM) coupling behaviours of natural and engineered barriers.

Up till now, many laboratory element tests have been conducted to investigate the basic thermo-mechanical behaviour of the geomaterials (e.g., Salager et al., 2008; Cui et al., 2009 and 2011; Zhang et al., 2010; Ye et al., 2015). Okada (2005 and 2006) reported that when the temperature increases, the strength of the geomaterials will decrease and the creep failure will occur more quickly. The volumetric change of the geomaterials, which was induced by heating, was also investigated by Baldi et al. (1991), Towhata et al. (1993), Laloui and Cekerevac (2003), Cekerevac and Laloui (2004). In order to get a better understanding of the above-mentioned THM behaviour of natural barrier, a lot of field heating experiments have been also conducted in the last decades (e.g., Muñoz, 2006; Gens et al., 2007 and 2009; Jia et al., 2007; Åkesson et al., 2009; Sawada et al., 2009; Gens, 2010). As a matter of fact, it is impossible to reproduce the whole process in the deep geological repository, only several hundreds of years within which significant thermal effects by HLW are expected is taken as the period we concern. Physically, even if the centrifuge model test is conducted, it could only reproduce the process for a few hundred years. Therefore, the numerical simulation is considered as a unique method to predict the above-mentioned THM behaviour and the long term stability of deep geological repository.

In this paper, firstly, in order to clarify the mechanical behaviour of the soft sedimentary rock under high temperature conditions, the thermal drained triaxial compression tests and the thermal drained triaxial creep tests were conducted under the room temperature (20°C), 40°C, 60°C and 80°C, respectively. Using these results, the element simulation based on the proposed model was also carried out. Then, a numerical simulation was conducted on the geological repository of HLW in two-dimensional scale, in which the host rock was supposed to be at saturated state. The performance of geological repository was numerically investigated in the simulations.

2. ELEMENT TESTS AND ITS SIMULATIONS

2.1 Element test under high temperature conditions

It is known that the homogeneity of a test specimen is a very important factor to acquire reliable results in element test, especially for understating the thermo-mechanical behaviour of the soft sedimentary rock. Tage stone, a typical soft volcanic tuff formed in Miocene age, is distributed widely in the Northeast Japan, and used as the specimen in this research. Zhang et al. (2010) pointed out that Tage stone is suitable for investigating the thermal properties of the soft sedimentary rock because its mineral matrix is chemically stable under high temperature conditions.

The cylindrical test specimen of Tage stone was 100 mm in height and 50 mm in diameter. In order to obtain a saturation state (more than 95% of the degree of saturation), saturation stage using vacuum pump was conducted. Using this specimen, the thermal drained triaxial compression and creep tests were conducted under temperatures of 20°C, 40°C, 60°C and 80°C respectively. The detailed testing condition of compression and creep tests are listed in Table 1 and Table 2.

Table 1 Scenario of thermal drained triaxial compression tests

Confining stress σ_r (MPa)	Temp. θ (°C)	Number of test
0.49	20	2
0.49	40	3
0.49	60	2
0.49	80	2
0.98	20	1
0.98	40	1
0.98	60	1
0.98	80	1
1.47	20	1
1.47	40	1
1.47	60	2
1.47	80	2

Note: Axial strain rate in loading is 0.002%/min.

In the creep tests, instead of abrupt loading, the axial creep load was applied at a constant rate until the specified creep stress was reached. The specified creep stress, which is defined as 95% of peak strength obtained from the thermal drained compression tests of 80°C, is listed in Table 2 as $q_{c0.95}$. In addition, the back pressures of 0.49 MPa were applied to the specimen in all tests to increase the degree of saturation. Test apparatus and more detailed information about tests procedure can be referred to the work by Zhang et al. (2010), Ye et al. (2015).

Table 2 Scenario of thermal drained triaxial creep tests

Confining stress σ_r (MPa)	Creep stress $q_{c0.95}$ (MPa)	Temp. θ (°C)	Number of test
0.49	7.37 (95%)	20	2
0.49	7.37 (95%)	40	1
0.49	7.37 (95%)	60	2
0.49	7.37 (95%)	80	2
0.98	9.10 (95%)	20	1
0.98	9.10 (95%)	40	1
0.98	9.10 (95%)	60	1
0.98	9.10 (95%)	80	2
1.47	9.98 (95%)	20	2
1.47	9.98 (95%)	40	1
1.47	9.98 (95%)	60	1
1.47	9.98 (95%)	80	1

Note: Axial loading rate is 0.05 kN/min.

Figure 1 shows the relationship between the deviator stress, the volumetric strain and the axial strain under different constant temperature in the thermal drained compression tests results. Figure 2 shows the relationship between the peak strength and the temperature. From these results, it is known that Tage stone exhibits a typical strain-softening and its volumetric strain firstly contracts and then turns to expand, so-called as dilatancy characteristics, in all tests. The temperature does influence the peak strength of Tage stone. The temperature fluctuation, however, does not affect the initial stiffness and the residual stress, the volumetric change both in qualitatively and quantitatively. If pay attention to the pressure dependency, it is found that as the confining stress increases, the peak strength and the residual stress also increase, while the volumetric strain at the residual state inhibits.

Figure 3 shows the time history of axial strain rate, volumetric strain under different constant temperature in the thermal drained creep tests results. Figure 4 shows the relationship between the creep failure time and the temperature. The time was set to zero at the beginning of shearing stage t_s or creeping stage t_c, after isotropic confining stress was applied. From these results, the general characteristics of creep behaviour, such as the primary or transient creep, the secondary or steady creep, and the tertiary or accelerating creep can be clearly observed. To compare the creep failure time under temperatures of 20°C and 80°C, except for the confining stress 0.98 MPa, it is strongly dependent on the temperature. In other words, the higher the temperature is, the faster the creep rupture will occur in most cases. It is admitted however, that there still exists some variation, which is dependent on the variation of characteristics with heating, in the creep failure time in all tests cases. Detailed discussion about this behaviour can be found in the references (Ye et al., 2015).

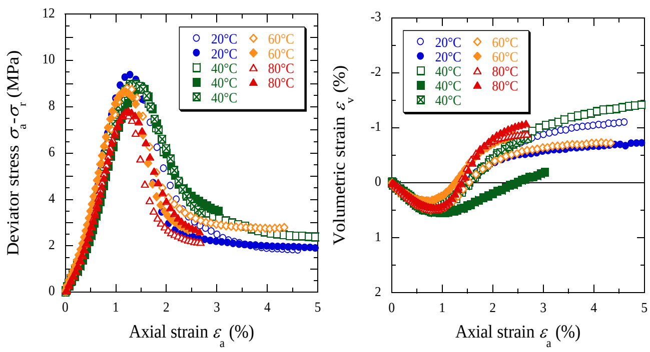

(a) Constant confining stress 0.49 MPa

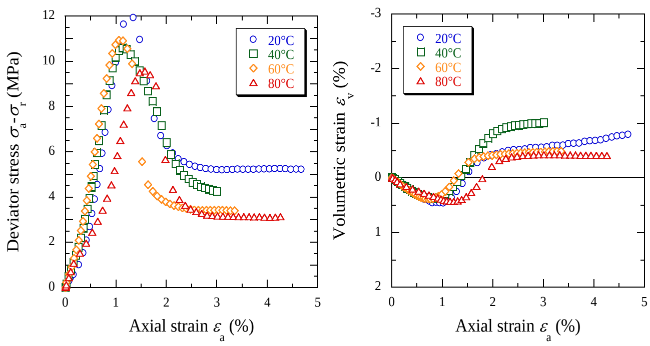

(b) Constant confining stress 0.98 MPa

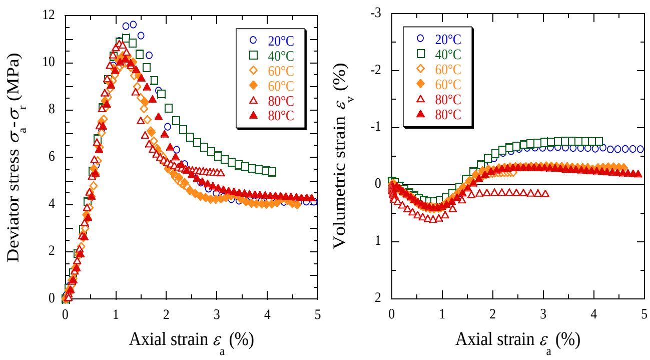

(c) Constant confining stress 1.47 MPa

Figure 1 Tests results of thermal drained compression tests under different constant temperatures

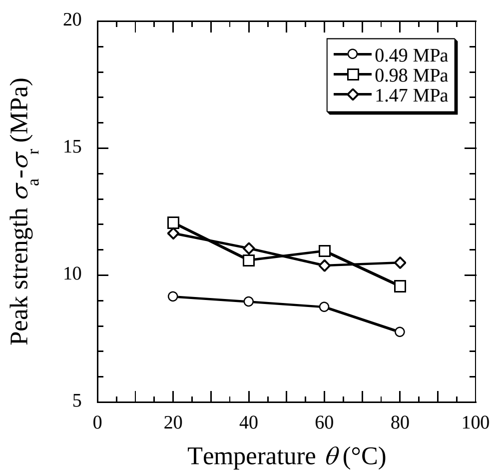

Figure 2 Relationship between peak strength and temperature obtained in thermal drained compression tests

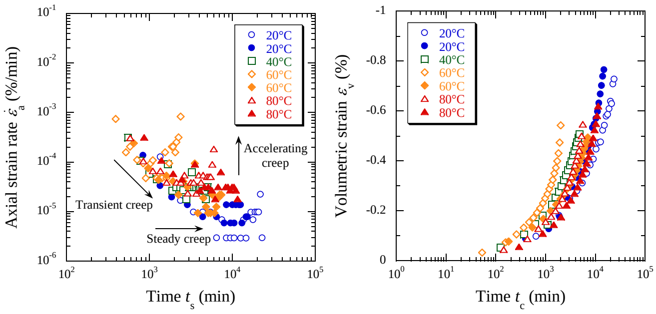

(a) Constant confining stress 0.49 MPa

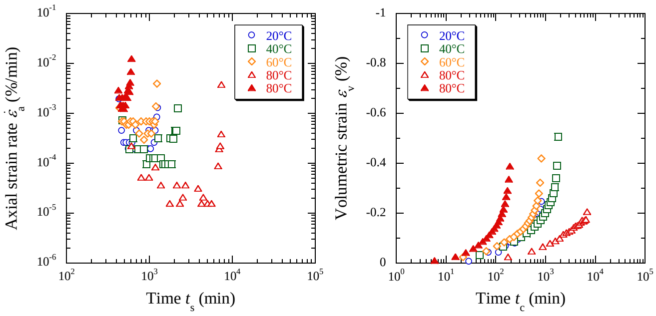

(b) Constant confining stress 0.98 MPa

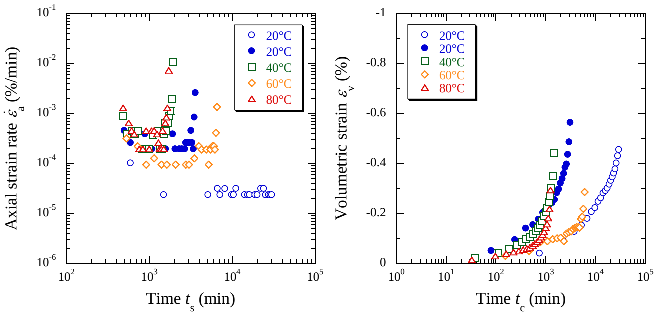

(c) Constant confining stress 1.47 MPa

Figure 3 Tests results of thermal drained creep tests under different constant temperatures

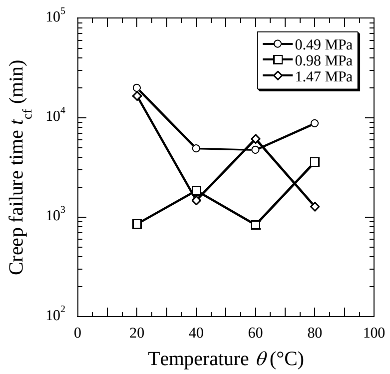

Figure 4 Relationship between creep failure time and temperature obtained in thermal drained creep tests

2.2 Element simulations based on the proposed model

Zhang et al. (2005) assumed that the soft sedimentary rock can be regarded as a heavily overconsolidated geomaterials, and proposed an elasto-viscoplastic model for the soft sedimentary rock using the concept of time dependency (Adachi et al., 1998), subloading yield surface (Hashiguchi and Ueno, 1977), and t_{ij} transformed stress space (Nakai and Mihara, 1984; Nakai and Hinokio, 2004). As the influence of temperature on the soft sedimentary rock is significantly (e.g., Okada, 2005 and 2006; Ye et al., 2015), a rational thermo-elasto-viscoplastic constitutive model was proposed (hereafter it will be called as the proposed model) based on previous model constructed in normal stress space (Zhang and Zhang, 2009; Xiong et al., 2014). In the works by Xiong et al. (2014), the plastic potential takes the same form as the work by Zhang et al. (2005), and is expressed as,

$$f(t_{ij},\varepsilon_v^p,\theta)=\ln\frac{t_N}{t_{N0}}+\varsigma(X)-\frac{1}{C_p}\left(\varepsilon_v^p-\frac{\rho}{1+e_0}\right)=0 \tag{1}$$

where, t_N is the modified mean effective stress in t_{ij} transformed stress space. X (= t_N / t_S) represents the shear stress ratio. t_{N0} is a reference mean stress and takes the value as 98 kPa. $C_p = (\lambda - \kappa) / (1 + e_0)$, where, λ is the compression index and κ is the swelling index. e_0 is an initial void ratio at $t_N = t_{N0}$ = 98 kPa under the isotropic normal consolidated condition. The evolution of void ratio difference ρ is written as in the following equation:

$$\frac{\rho}{1+e_0}=-\Lambda\frac{G(\rho,t)}{t_N+3K\alpha_T^s(\theta-\theta_0)}+h(t) \tag{2}$$

where, K is the bulk modulus of solid phase. α_T^s is the thermal expansion coefficient of solid phase whose value should be negative because the compression is usually taken as positive in the geomechanics. θ is the present temperature, θ_0 the reference temperature, which is an arbitrary value, is taken as the global average temperature 15°C.

$$h(t)=\varepsilon_v^0(1+t/t_1)^{-\alpha} \tag{3}$$

$$G(\rho,t)=a\cdot\rho\cdot\rho^{C_n\ln(1+t/t_1)} \tag{4}$$

where, ε_v^0 is an initial volumetric strain rate at time t = 0, which represents the time when the shearing begins. t_1 is a unit time and used to standardized the time, and always takes the value of 1.0. α is the time dependent parameter that controls the gradient of strain rate vs. time in logarithmic axes during the creep tests. C_n controls the strain rate dependency. a is the fitting parameter, and controls the losing rate of overconsolidation ratio.

Nine parameters are involved in the proposed model, among which λ, κ, R_f, N and ν are exactly the same as in the Cam-clay model (Roscoe et al., 1963; Schofield and Wroth, 1968). The other four parameters, which a, α, C_n, β, are the same as the model proposed by Zhang et al. (2005). These parameters have clear physical meanings and can be determined by the triaxial compression and creep tests. A detailed description of calibration method for these nine parameters can be found in Zhang et al. (2005). To describe thermo-mechanical behaviour of the geomaterials, only the thermal expansion coefficient α_T^s, which is a physical parameter with a value that is fixed for a given geomaterial, is added into the model proposed by Zhang et al. (2005).

In order to check the performance of proposed model, some typical mechanical and thermodynamic behaviour of Tage stone in the thermal drained triaxial compression and creep tests were simulated. The material and physical parameters of Tage stone based on the simulation of element tests is listed in Table 3. It should be emphasized that except for the value of stress ratio at critical state R_f, all parameters used in the proposed model were unified under different confining pressures. Conditions of element simulations were the same as the element test's ones. Underlined parameters were also used in the later discussion, which in THM analysis of two-dimensional scale.

Table 3 Material parameters and physical parameters of Tage stone for the element simulations

Parameters	Unit	Value
Plastic stiffness $\boldsymbol{E_p}$ (= λ - κ)	-	<u>0.015</u>
Critical state stress ratio $\boldsymbol{R_f}$	-	6.9 (0.49 MPa) 6.0 (0.98 MPa) 5.5 (1.47 MPa)
Void ratio $\boldsymbol{N}$ (p = 98 kPa on *N.C.L.*)	-	<u>0.5</u>
Poisson's ratio $\boldsymbol{\nu}$	-	<u>0.12</u>
Young's modulus $\boldsymbol{E}$	MPa	<u>1000</u>
Degradation parameter of overconsolidation state $\boldsymbol{a}$	-	<u>3000</u>
Time dependent parameter $\boldsymbol{\alpha}$	-	<u>0.5</u>
Time dependent parameter $\boldsymbol{C_n}$	-	<u>0.025</u>
Parameter for plastic potential shape $\boldsymbol{\beta}$	-	<u>1.1</u>
Thermal expansion coefficient of solid phase $\boldsymbol{\alpha_T^s}$	K^{-1}	<u>-1.5E-5</u>
Initial degree of overconsolidation ratio ***OCR***	-	40.0 (0.49 MPa) 20.0 (0.98 MPa) 13.3 (1.47 MPa)
Temperature $\boldsymbol{\theta}$	°C	20, 40, 60, 80
Axial strain rate $\dot{\varepsilon}_a$	%/min	0.002
Creep stress $\boldsymbol{q_{c0.95}}$	MPa	8.34 (0.49 MPa) 10.31 (0.98 MPa) 11.07 (1.47 MPa)

Figure 5 shows the simulated results of Tage stone in the thermal drained compression and creep tests under different constant temperature during shearing stage or creeping stage. Figure 6 shows the relationship between the calculated peak strength, creep failure time and the temperature. It is verified that the proposed model can not only describe the compression tests but also the creep tests in their overall behaviour, that is the strain-softening behaviour and dilatancy characteristics, and the pressure, the time, the temperature dependencies, with a set of unified parameters in qualitatively. However, the difference between the reductions in peak strength due to heating is small as the confining stress increases, as shown in Figure 6. This is because that in the element simulations, the influence of thermal expansion coefficient is relatively lower under higher the confining stress.

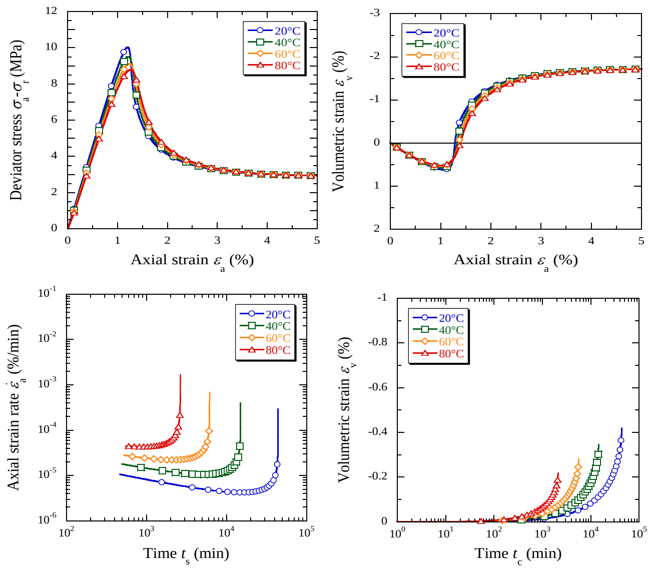

(a) Constant confining stress 0.49 MPa

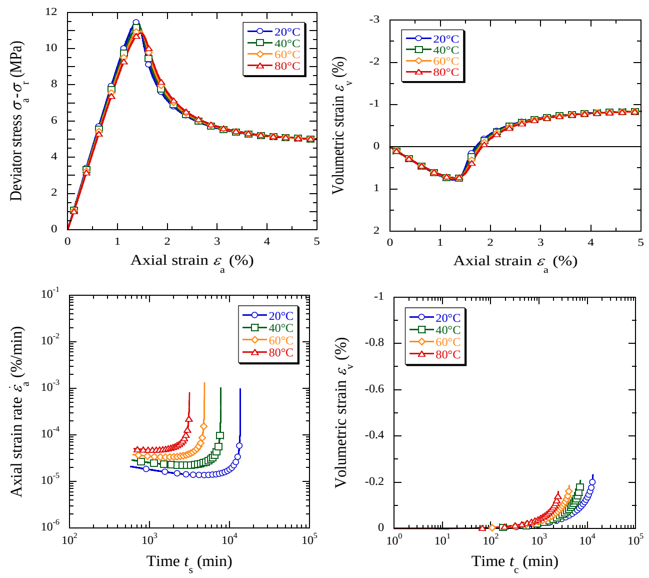

(b) Constant confining stress 0.98 MPa

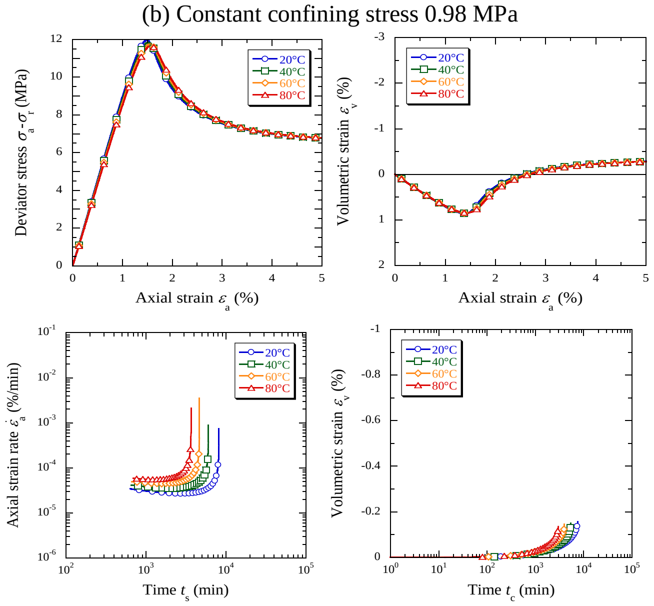

(c) Constant confining stress 1.47 MPa

Figure 5 Simulations of thermal drained compression and creep tests under different constant temperatures

3. THM ANALYSIS OF TWO-DIMENTIONAL SCALE

The numerical simulations reproducing the deep geological repository (2D) were conducted with a FEM program named as ***SOFT*** (Xiong et al., 2014), adopting unified field equations for thermo-hydraulic-mechanical-air (THMA) coupling behaviours of the geomaterials and using finite element-finite difference (FE-ED) scheme for soil-water-air three phase coupling problem. Note, however, that the effect of air was not taken into account in this simulation. A durative time was set to 300 years (3 years / STAGE). In this simulation, the distance from the targeted points to the surface of HLW was 0 m (No.01), 2 m (No.02), 5.4 m (No.03), 10.7 m (No.04), 26.7 m (No.05), 96.8 m (No.06) and 154.1 m (No.07) respectively in horizontal direction, as shown in Figure 7.

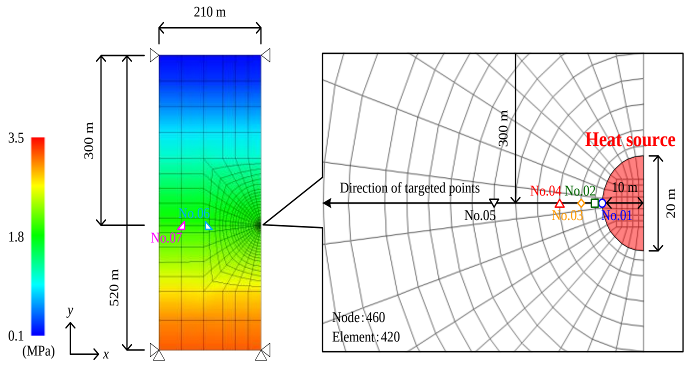

Figure 7 2D FEM mesh and distribution of effective mean stress at initial gravitational stress field

Considering the symmetric geometry and loading conditions, only a half area was considered in this simulation. Figure 7 shows two-dimensional finite element mesh, in which the area was a rectangle of 210 m x 520 m. For simplify, HLW was regarded as circle with 20 m in diameter, and the center of circle was located at the place 300 m below the ground surface (Japan Nuclear Cycle Development Institute, 2000). As to the displacement boundary conditions, the bottom of domain was set to be fixed in the vertical direction, while the two side boundaries were set to be free in the vertical direction, and fixed in the horizontal direction. The initial stress field was calculated by gravitational force. The hydraulic boundary conditions of bottom, two side boundaries, and all surfaces of HLW were set as undrained condition. The initial total water head was given as 520 m.

For the thermal condition, the initial temperature of whole considered area was set to be 20°C. The ground surface was always kept 20°C all time and the heat insulation was assumed for other three sides. The heat was assumed to be generated by HLW which had been cooled in the facility on the ground surface before being buried. Considering the time of ventilation, two cases were set in this simulation; one was 10 years as Case A, and the other was 100 years as Case B. In the KBS-3 concept, the volume of HLW occupies about 1.6% of the whole tunnel space. Therefore, in this simulation, only 1.6% of heat emission was applied for both cases as those in the work by Thunvik and Braester (1991), as shown in Figure 8.

The host rock was considered as the soft sedimentary rock at saturated state. Its mechanical behaviour was reproduced using the propose model. The technological and engineering barriers were assumed to be the elastic material, and the parameters of materials used in this simulation were listed in Table 3 and Table 4.

Figure 9 shows the distribution of temperature and its time histories at targeted points in Case A and Case B. From these results, it is known that the temperature increases initially due to heat emission of HLW. The temperature of No.01 located on the surface of HLW is obviously very high, maximum around 150°C in Case A, and the peak temperatures of targeted points decrease with distance from HLW. In Case A, the temperature begins to decrease during 30-150 years, and cools down to a certain value. However, the temperature does not exhibit a tendency to a steady state within the simulation time. Meanwhile, in Case B, the peak temperatures of all targeted points are below 80°C, and show a trend of a steady state.

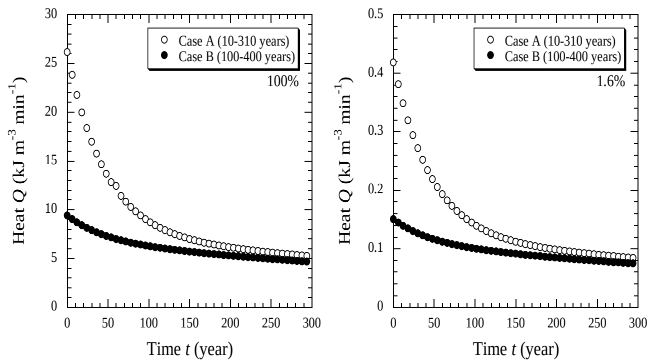

Figure 8 Time history of heat emission in HLW at practical field project

Table 4 Material parameters and physical parameters of host rock and heat source for boundary value problem

Parameters	Unit	Value
Critical state stress ratio R_f	-	5.5
Permeability k	m min^{-1}	1.0E-9
Thermal expansion coefficient of fluid phase α_T^f	K^{-1}	-2.07E-4
Specific heat of solid phase c^s	J kg^{-1} K^{-1}	840
Specific heat of fluid phase c^f	J kg^{-1} K^{-1}	4184
Thermal conductivity of solid phase k_T^s	kJ m^{-1} K^{-1} min^{-1}	0.2 (Hr) 20 (Hs)
Heat transfer coefficient of air boundary α_c	kJ m^{-2} K^{-1} min^{-1}	236
Soil particle density ρ_s	Mg/m^3	2.56
Consolidation yield stress p_c	MPa	19.6

Hr: Host rock, Hs: Heat source.

Figure 10 shows the distribution of total water head at specified time. The total water head in two cases increase due to the build-up of excess pore water pressure as the increasing of temperature. And later, the excessive water pressure is allowed to dissipate with time, and reaches to the hydrostatic pressure eventually. In this simulation, the total water head at 300 years is higher than initial value 520 m because all boundaries except for the ground surface were set as undrained condition.

Figure 11 and Figure 12 show the distribution of deviator strain $\sqrt{2I_2}$ and volumetric strain at specified time, respectively. Here, I_2 is the second invariant of deviator strain tensor. See Figure 11, it can be seen that the maximum deviator strain occurs in the area of 45° from the horizontal direction. Meanwhile, the volumetric strain of all targeted points is expansion in two cases. Even the proposed model used in this simulation was introduced only the thermal expansion coefficient to describe the temperature dependency, the contractive volumetric strain occurs in some areas because of the displacement boundary condition.

To compare the simulations results between Case A and Case B, it is found that the increment of total water head, deviator strain, and volumetric strain in Case A is much higher than that in Case B due to the difference in heat emission.

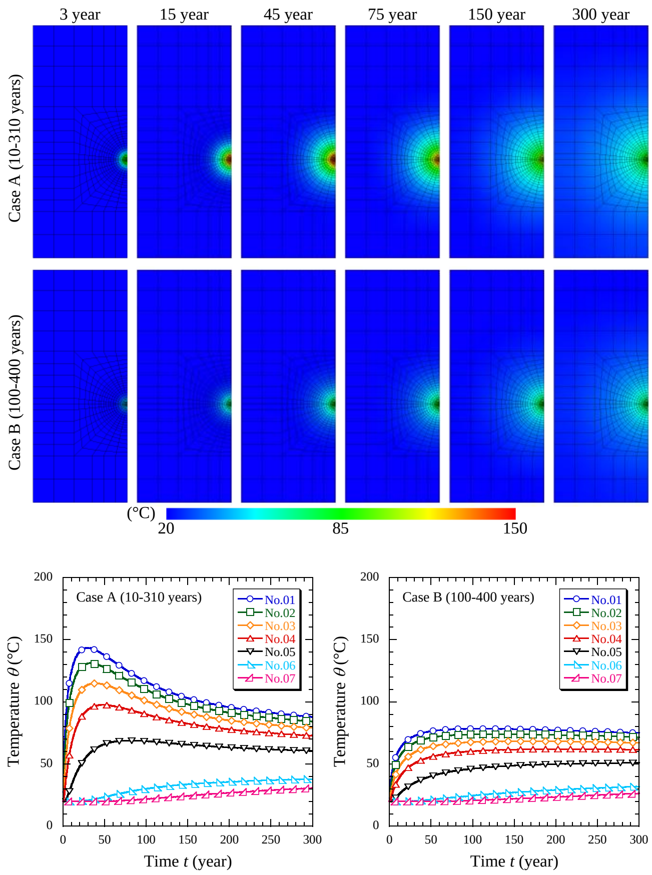

Figure 9 Distribution of temperature and its time histories at targeted points in Case A, Case B

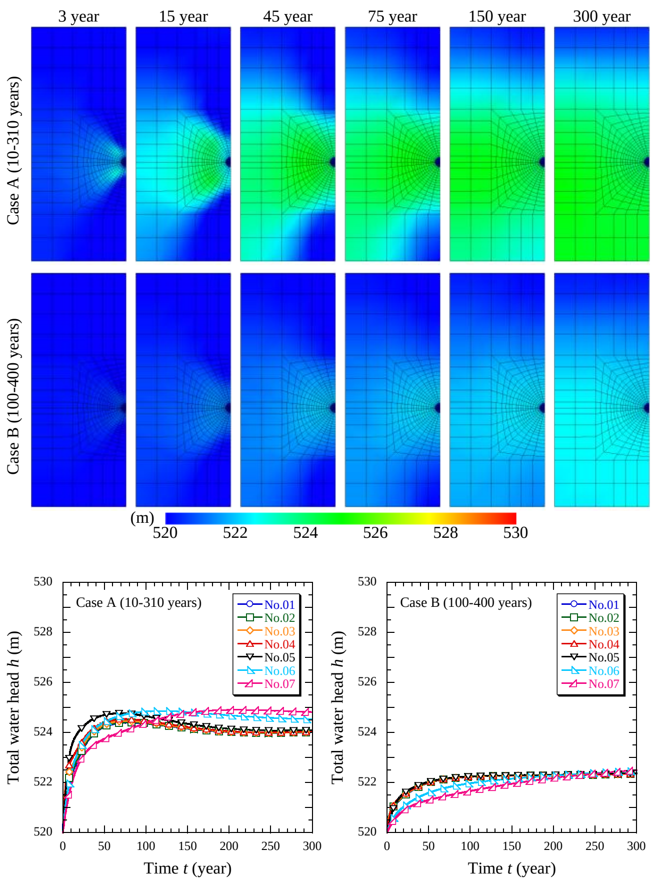

Figure 10 Distribution of total water head and its time histories at targeted points in Case A, Case B

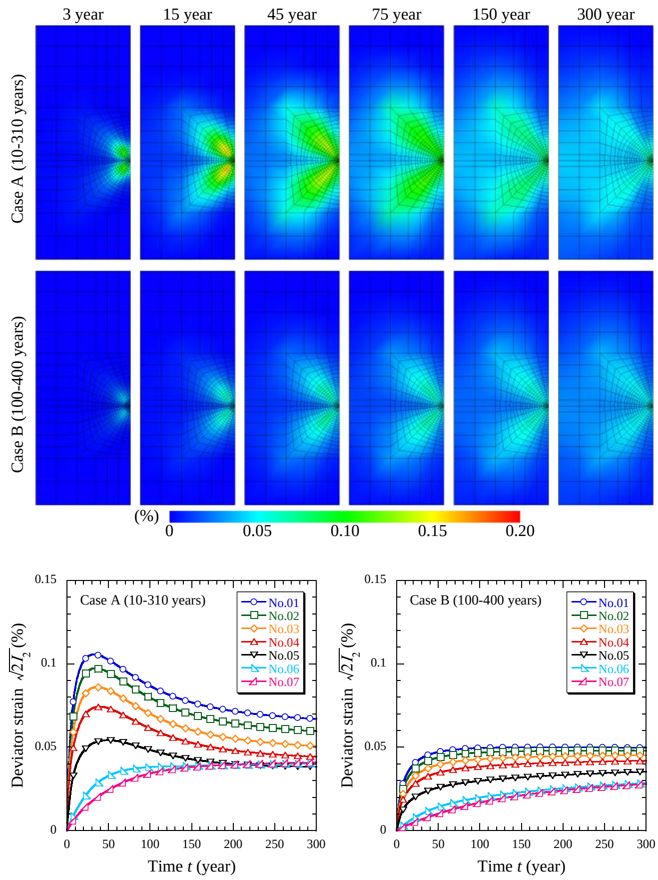

Figure 11 Distribution of deviator strain and its time histories at targeted points in Case A, Case B

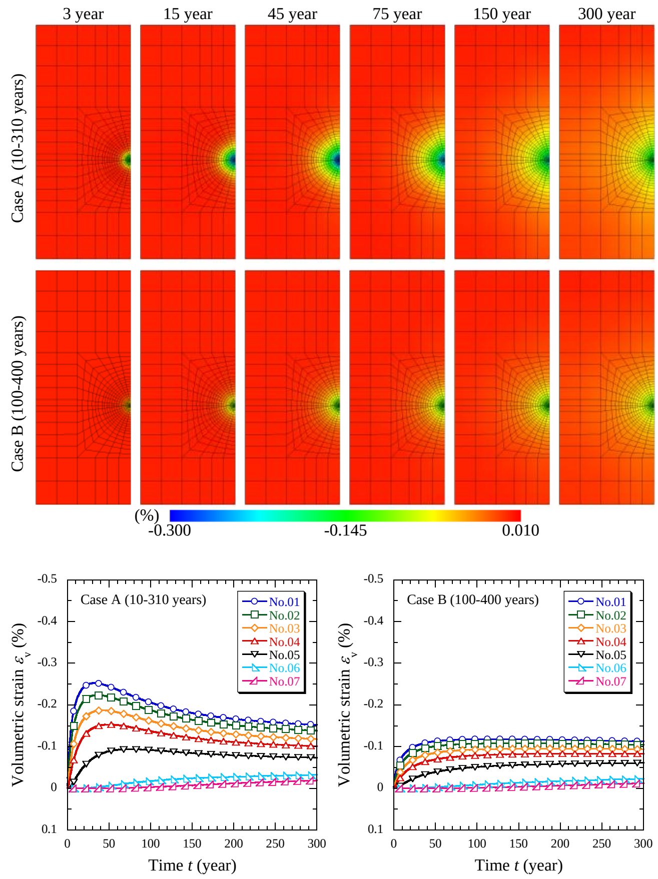

Figure 12 Distribution of volumetric strain and its time histories at targeted points in Case A, Case B

4. CONCLUSION

In this paper, to understand the fundamental thermo-mechanical behaviour of the soft sedimentary rock as a potential candidate for the host rock in Japan, the thermal drained triaxial compression and creep tests have been conducted under different constant temperatures. And then, the element simulations based on the proposed thermo-elasto-viscoplastic constitutive model and its application to THM analysis on a two-dimensional scale repository project have been also carried out. The following concluding remarks can be drawn:

1. In the triaxial compression tests, the peak strength of Tage stone decreases as the temperature increase, and the volumetric strain in all tests firstly contracts and then expands. In the triaxial creep tests, the creep failure occurs more quickly as the temperature increase. In other words, the temperature does influence the peak strength and the creep failure time of Tage stone at element level.
2. In the element simulations, it is proved that the proposed model can describe the mechanical behaviours of the soft sedimentary rock under different temperatures with a rather satisfactory accuracy on the whole. It is also found that the simulation can quantitatively describe the THM coupling behaviours of the geomaterials in the geological repository of HLW, such as the difference of heat source, the change of temperature, the migration of excess pore water and the deformation of natural barrier. In addition, the cooling period before the geological repository of HLW is also very important to the safety of not only the natural barrier but also the engineered barrier.

5. REFERENCES

Adachi, T., Oka, F., and Zhang, F. (1998) "An elasto-viscoplastic constitutive model with strain softening". Soils and Foundations, 38, Issue 2, pp27-35.

Åkesson, M., Jacinto, A. C., Gatabin, C., Sanchez, M., and Ledesma, A. (2009) "Bentonite THM behaviour at high temperatures: experimental and numerical analysis". Géotechnique, 59, Issue 4, pp307-318.

Baldi, G., Hueckel, T., Peano, A., and Pellegrini, R. (1991) "Developments in modelling of thermo-hydro-geomechanical behaviour of Boom clay and clay-based buffer materials". Commission of the European Communities, Nuclear science and technology, Report EUR 13365.

Cekerevac, C., and Laloui, L. (2004) "Experimental study of thermal effects on the mechanical behaviour of a clay". International journal for Numerical and Analytical Methods in Geomechanics, 28, Issue 3, pp209-228.

Cui, Y. J., Le, T. T., Tang, A. M., Delage, P., and Li, X. L. (2009) "Investigating the time-dependent behaviour of Boom clay under thermo-mechanical loading". Géotechnique, 59, Issue 4, pp319-329.

Cui, Y. J., Tang, A. M., Qian, L. X., Ye, W. M., and Chen, B. (2011) "Thermal-mechanical behavior of compacted GMZ Bentonite". Soils and Foundations, 51, Issue 6, pp1065-1074.

Gens, A., Vaunat, J., Garitte, B., and Wileveau, Y. (2007) "In situ behaviour of a stiff layered clay subject to thermal loading: observations and interpretation". Géotechnique, 57, Issue 2, pp207-228.

Gens, A., Sánchez, M., Guimarães, L. Do N., Alonso, E. E., Lloret, A., Olivella, S., Villar, M. V., and Huertas, F. (2009) "A full-scale in situ heating test for high-level nuclear waste disposal: observations, analysis and interpretation". Géotechnique, 59, Issue 4, pp377-399.

Gens, A. (2010) "Soil-environment interactions in geotechnical engineering". Géotechnique, 60, Issue 1, pp3-74.

Hashiguchi, K., and Ueno, M. (1977) "Elastoplastic constitutive laws of granular materials, Constitutive Equations of Soils". Proceedings of the 9th International Conference on Soil Mechanics and Foundations Engineering, Special Session 9, Tokyo, Japan, JSSMFE, pp73-82.

Japan Nuclear Cycle Development Institute (2000) "H12: Project to establish the scientific and technical basis for HLW disposal in Japan -Second progress report on research and development for the geological disposal of HLW in Japan-".

Jia, Y., Wileveau, Y., Su, K., Duveau, G., and Shao, J. F. (2007) "Thermo-hydro-mechanical modelling of an in situ heating experiment". Géotechnique, 57, Issue 10, pp845-855.

Laloui, L., and Cekerevac, C. (2003) "Thermo-plasticity of clays: An isotropic yield mechanism". Computers and Geotechnics, 30, Issue 8, pp649-660.

Muñoz, J. J. (2006) "Thermo-hydro-mechanical analysis of soft rock. Application to a large scale heating test and large scale ventilation test". Universitat Politècnica de Catalunya, PhD thesis.

Nakai, T., and Mihara, Y. (1984) "A new mechanical quantity for soils and its application to elastoplastic constitutive models". Soils and Foundations, 24, Issue 2, pp82-94.

Nakai, T., and Hinokio, M. (2004) "A simple elastoplastic model for normally and over consolidated soils with unified material parameters". Soils and Foundations, 44, Issue 2, pp53-70.

Okada, T. (2005) "Mechanical properties of sedimentary soft rock at high temperatures (Part 1) -Evaluation of temperature dependency based on triaxial compression test-". Central Research Institute of Electric Power Industry, Civil Engineering Research Laboratory, Report No. N04026 (in Japanese).

Okada, T. (2006) "Mechanical properties of sedimentary soft rock at high temperatures (Part2) -Evaluation of temperature dependency of creep behavior based on unconfined compression test-". Central Research Institute of Electric Power Industry, Civil Engineering Research Laboratory, Report No. N05057 (in Japanese).

Roscoe, K. H., Schofield, A. N., and Thurairajah, A. (1963) "Yielding of clays in states wetter than critical". Géotechnique, 13, Issue 3, pp211-240.

Salager, S., François, B., El Youssoufi, M. S., Laloui, L., and Saix, C. (2008) "Experimental investigations of temperature and suction effects on compressibility and pre-consolidation pressure of a sandy silt". Soils and Foundations, 48, Issue 4, pp453-466.

Sawada, M., Okada, T., Tani, K., Takakura, N., and Ikenoya, T. (2009) "In-situ heating test in the sedimentary soft rock (Part 2) -Application of thermo-hydro-mechanical coupled analysis to the sedimentary soft rock-". Central Research Institute of Electric Power Industry, Civil Engineering Research Laboratory, Report No. N08055 (in Japanese).

Schofield, A. N., and Wroth, C. P. (1968) "Critical State Soil Mechanics". McGraw-Hill.

Thunvik, R., and Braester, C. (1991) "Heat propagation from a radioactive waste repository (SKB 91 reference canister)". SKB Technical Report 91-61.

Towhata, I., Kuntiwattanaku, P., Seko, I., and Ohishi, K. (1993) "Volume change of clays induced by heating as observed in consolidation tests, Soils and Foundations, 33, Issue 4, pp170-183.

Xiong, Y., Zhang, S., Ye, G., and Zhang, F. (2014) "Modification of thermo-elasto-viscoplastic model for soft rock and its application to THM analysis of heating tests". Soils and Foundations, 54, Issue 2, pp176-196.

Ye, G., Nishimura, T., and Zhang, F. (2015) "Experimental study on shear and creep behaviour of green tuff at high temperatures". International Journal of Rock Mechanics and Mining Sciences, 79, pp19-28.

Zhang, F., Yashima, A., Nakai, T., Ye, G. L., and Aung, H. (2005) "An elasto-viscoplastic model for soft sedimentary rock based on tij concept and subloading yield surface". Soils and Foundations, 45, Issue 1, pp65-73.

Zhang, S., and Zhang, F. (2009) "A thermo-elasto-viscoplastic model for soft sedimentary rock". Soils and Foundations, 49, Issue 4, pp583-595.

Zhang, S., Nakano, H., Xiong, Y., Nishimura, T., and Zhang, F. (2010) "Temperature-controlled triaxial compression/creep test device for thermodynamic properties of soft sedimentary rock and corresponding theoretical prediction". Journal of Rock Mechanics and Geotechnical Engineering, 2, Issue 3, pp255-261.